

# Modeling Strain-Encoded (SENC) MRI for Use in Clinical Breast Imaging

A. A. Harouni<sup>1</sup>, N. F. Osman<sup>2</sup>, and M. A. Jacobs<sup>3</sup>

<sup>1</sup>Electrical and Computer Engineering, Johns Hopkins University, Baltimore, Maryland, United States, <sup>2</sup>Department of Radiology, Johns Hopkins University, Baltimore, Maryland, United States, <sup>3</sup>Department of Radiology and Oncology, Johns Hopkins University school of medicine, Baltimore, Maryland, United States

**Introduction:** Breast cancer tumors are 3-13 times stiffer than normal tissue [1]. The use of strain-encoded (SENC) MRI was proposed in [2] to detect masses by measuring strain, which is inversely proportional to stiffness. The use of strain imaging of breast lesions would provide a new measure for clinical diagnosis between benign and malignant tissue. Previously in [2], we have shown that SENC can detect tumors in ex-vivo tissue by applying 30% compression. However, 30% compression was inherited from SENC origin [3], as SENC was initially developed to image the myocardial circumferential strain (range +5% to -30%). For breast imaging, multiple 30% compressions obstruct applying SENC in a clinical setting. In this work, we determine the minimum amount of compression required to detect and classify masses using finite element method (FEM) simulations and phantom studies.

**Methods:** We developed FEM to simulate the tissue's deformation after compression in order to understand relationship between stiffness and strain under different compressions. We simulated a cross section of a phantom using 31x55 nodes connected together by constant strain triangles having linear shape function. Fixed boundary conditions were used to mimic the compression performed, tissue was assumed to have constant thickness with Poisson ratio of 0.49. To acquire SENC strain images, we used the hardware described in [2] to periodically apply different compression (CMP) and relaxation (REX) levels. In SENC [3], we apply tagging preparation pulses to the tissue while being relaxed/compressed, then acquire SENC-CMP/SENC-REX images after the tissue is fully compressed/relaxed. SENC relies on tagging deformation during compression or relaxation to measure the strain.

**Materials:** A custom-made phantom with five groups of masses was designed to determine SENC sensitivity to different stiffness for different compression levels. Groups A, B, C, and D were harder than the background, while group E was softer than the background. All masses were cuboids 10mm thickness with varying sizes (3-12mm) as shown in Fig.1. We used a dynamic mechanical analyzer to determine material's stiffness, which were 593, 226, 171, 100, 20 and 71KPa for groups A, B, C, D, E and background, respectively. Samani *et al* [1], examined 169 fresh ex-vivo breast tissue containing different types of cancer masses. Comparing their results with our masses' stiffness, our phantom mimics malignant tumors (group A), benign masses (groups B & C), and normal tissue (groups D & E).

**Experiments:** We performed our scans on a 3T MRI Philips scanner (Philips Medical Systems, Best, the Netherlands) using a four-channel phased-array breast coil. All scans had FOV=192x192mm<sup>2</sup>, in-plane resolution=1x1mm<sup>2</sup>, slice thickness=5mm. We performed T1W (TR=495/TE=10ms) and T2W spin echo (TR=2500/TE=60ms) scans. SENC scans used segmented Cartesian K-space acquisition (TFE=10). We performed 7%, 10%, 16% and 23% compression and 8%, 11%, 18% and 29% relaxation. For visualization, we unified all color pallets such that masses that have low strain values would be colored in red, while normal background is colored in blue for both SENC-CMP and SENC-REX images. Masses were manually segmented and contrast-to-noise elastography ratio (CNR<sub>e</sub>) was calculated.

**FEM results:** Fig. 2a shows a diagram for FEM simulations of our phantom's cross section with five masses (2, 4, 6, 8 and 10mm) at 10% compression with the corresponding strain profile along green, red, and blue slices (Fig. 2b). Note that strain at the blue slice (furthest from the masses) remains constant around -11%, while the strain profile at the green slice (intersecting with the masses) varies from -10% (within the background outside the masses) to -2% (within the masses). Strain inside the masses depends upon the length of the mass (see dotted black arrows in Fig. 2b). Note that the strain profile of the red slice (directly behind the masses) appears to be mirroring the strain profile of the green slice (Fig. 2b). This is because the stiff masses are pushing against the soft tissue behind them.

**Phantom results:** Masses of all groups (A-E) were visual on T1W and T2W images (not shown). Figs. 2d-f show SENC-CMP and SENC-REX images at two slice position: directly behind (c & e) and intersecting (d & f) the masses. Arrows point to the tissue behind the masses, which is compressed more than the applied external compression. This confirms the FEM results and increases the confidence of mass detection using SENC MRI. Fig. 3 shows SENC-CMP (a & c) and SENC-REX (b & d) for different compression and relaxation levels. Table 1 shows strain (mean±SD) for masses manually segmented from SEN-CMP and SENC-REX images. Using SENC-CMP (at -7%) and SENC-REX (at 8% & 11%) images, we detected both malignant (group A) and benign (groups B & C) but not normal (groups D & E) masses; therefore, differentiating normal from suspicious masses. However, these images had moderate CNR<sub>e</sub> (11-20) and suffered from rim artifacts due to imperfect compressions. Using strain values from SENC-CMP10% and SENC-REX18% with high CNR<sub>e</sub> (60&30), we could differentiate between malignant (strain =-5.1 & 5.5) and benign masses (strain=-8.2, -8.8 & 9.7, 10.4).

**Conclusion:** Results show that SENC is capable of detecting both benign and malignant masses using low compressions (<7%). However, to differentiate between them higher compression (10%-15%) is needed. Therefore, for maximum patient comfort, we propose to start with small compressions then progress to larger compressions when masses are detected at the scanner console. Thus, combining SENC with breast MRI could increase the specificity of diagnosis.

**References:** [1] Samani *et al*, Phys. Med. Biol. 52:1565 (2007). [2] Harouni *et al*, Academic radiology, in-press (2011). [3] Osman N. *et al*, MRM 46:324-10 (2001).

**Acknowledgment:** This work was supported in part by the following grants NHLBI R01HL072704, NIH 1P50HL08946, 1R01CA100184, and P50 CA103175.

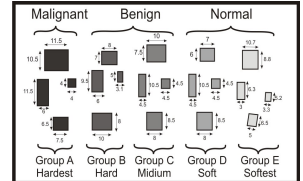


Fig.1: Phantom sketch diagram

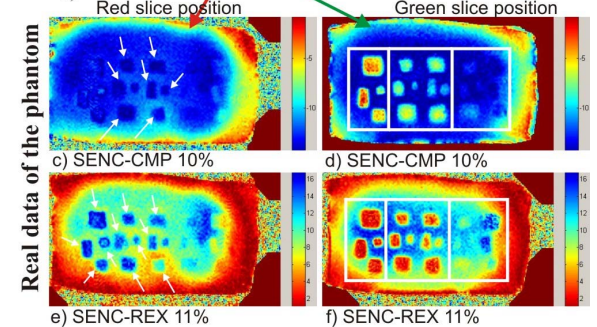
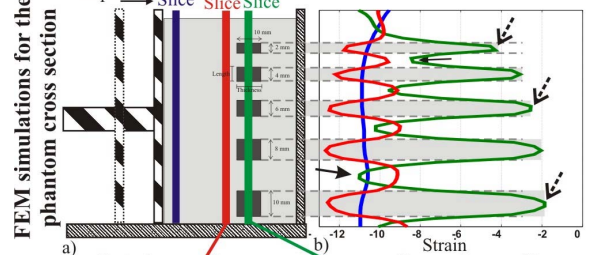


Fig.2: a) FEM simulation compressing the phantom by 10%. b) Strain profile at green, red and blue slices calculated from FEM. SENC-CMP images (c,d) and SENC-REX images (e,f) acquired at slices that contain masses (d,f) and positioned immediately behind the masses (c,e) corresponding to the green and red slices in FEM simulations, respectively. White arrows point to masses.

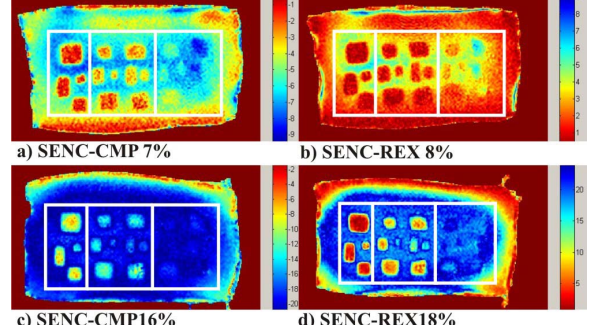


Fig.3: SENC images for different compression & relaxation levels. White rectangles separate malignant, benign, and normal masses.

	SENC Compression (SENC-CMP)				SENC Relaxation (SENC-REX)			
	-7%	-10%	-16%	-23%	+8%	+11%	+18%	+29%
Grp A	-3.0±1.0	-5.1±1.7	-10.5±2.6	-13.4±5.0	1.1±0.8	3.3±1.8	5.5±4.3	8.1±5.9
Grp B	-3.7±0.9	-8.2±1.3	-14.5±2.0	-18.1±4.5	1.3±0.8	4.5±1.9	9.7±3.3	15.2±5.5
Grp C	-3.9±0.9	-8.8±1.6	-15.0±2.4	-20.1±3.9	1.4±0.8	4.8±1.8	10.4±3.6	15.7±6.4

Table 1: Strain (mean±SD) for SENC-CMP and SENC-REX under different compression and relaxation levels.